Werk

Jahr: 1975
Kollektion: fid.geo
Signatur: 8 Z NAT 2148:41
Digitalisiert: Niedersächsische Staats- und Universitätsbibliothek Göttingen
Werk Id: PPN1015067948_0041
PURL: http://resolver.sub.uni-goettingen.de/purl?PPN1015067948_0041

LOG Id: LOG_0087
LOG Titel: Wave and particle observations by Explorer 45 pertaining to wave-particle interactions
LOG Typ: article

Übergeordnetes Werk

Werk Id: PPN1015067948
PURL: http://resolver.sub.uni-goettingen.de/purl?PPN1015067948
OPAC: http://opac.sub.uni-goettingen.de/DB=1/PPN?PPN=1015067948

Contact

Niedersächsische Staats- und Universitätsbibliothek Göttingen
Georg-August-Universität Göttingen
Platz der Göttinger Sieben 1
37073 Göttingen
Germany
Email: gdz@sub.uni-goettingen.de

J. Geophys. 41, 551 – 580, 1975

REVIEW ARTICLE

Wave and Particle Observations by Explorer 45 Pertaining to Wave-Particle Interactions*

T.A. Fritz and D.J. Williams

U.S. Department of Commerce, National Oceanic and Atmospheric Administration
Environmental Research Laboratories, Boulder, Colorado 80302, USA

Abstract. We present a review of results obtained from the NASA Small Scientific Satellite (Explorer 45) concerning wave and particle observations which pertain to wave-particle interactions near the equatorial plane out to radial distances of 5.2 R_E (earth radii). We first outline observations which confirm some preexisting ideas concerning various magnetospheric processes such as the "injection" of particles during substorms, the existence of ELF hiss throughout the region of the plasmasphere, and the role which convection plays in explaining the overall gross motions of the particle dynamics. In the second part of the review we examine observations from Explorer 45 pertaining to magnetospheric processes and mechanisms around which there still exists a good deal of uncertainity. We comment upon the nature of the substorm injection process, and mechanism producing the ELF plasmaspheric hiss, and the role the various competing processes play in the decay of the storm-time ring current.

Key words: Magnetosphere – Wave and Particle Observations – Explorer 45.

I. Introduction and Description of Explorer 45

The subject of wave-particle interactions inside the magnetosphere has become an increasingly active area of research in recent years. We wish to present a short review and compilation of observations made by the NASA Small Scientifice Satellite (S^3), Explorer 45, of waves and particles, near the equatorial plane

* Invited paper presented at the European Geophysical Society Symposium on Plasma Instabilities and Wave Particle Interactions in the Magnetosphere, Trieste, Italy, September 23–25, 1974. The paper is being published as a contribution to a collection honoring Professor G. Pfotzer of the Max-Planck-Institut für Aeronomie, Lindau/Harz, Germany.

in the inner magnetosphere ($L \leqq 5$) which pertain to concepts of wave-particle interactions. Explorer 45 was launched on 15 November 1971 into an elliptical orbit having an apogee of 5.24 earth radii, a perigee of 220 km, a period of 7.82 hours and an inclination of 3.5°. An electrostatic analyzer-channelton instrument plus three separate solid-state detector systems measure proton intensities from 0.73 keV to 2800 keV in 31 differential energy channels and electron intensities from 0.73 to 560 keV in 20 steps. A complete description of the Explorer 45 sattelite and program has been presented by Longanecker and Hoffman (1973).

The satellite spin axis is maintained in the plane of the orbit and pitch angle information is obtained by sectoring the satellite spin (8.451 seconds) into 32 segments. All pitch angles presented here are measured pitch angles using simultaneous data from the on-board 3 axis flux gate magnetometer. Single axis DC electric field measurements are made perpendicular to the spin axis along with AC electric field noise from 0.3 Hz to 100 kHz (19 band pass channels). Two axis search coil magnetometers provide magnetic noise measurements from 1 Hz to 3 kHz in 7 band pass channels. In addition to the band pass measurements both electric and magnetic noise measurements are passed through a broadband (100 Hz to 10 kHz) filter and telemetered separately over a wideband transmitter (Longanecker and Hoffman, 1973). The location of the plasmapause can be identified by using the saturation characteristics of the DC electric fields experiment (Maynard and Cauffman, 1973) and is believed to represent a cold plasma number density of 60 to 100 particles/cm^3 (Maynard, personal communication).

The S^3 concept is unique. The satellite is considered as a single experiment. In keeping with this concept, copies of a single data tape, containing all data, are distributed to each experimenter in the program. With this operational situation and the strong cooperation of the experimenter team members, magnetospheric problems can be viewed and approached with the complete S^3 set of simultaneous data bearing on the problem and the compilation of results can be assembled into review papers such as the present one early in the data analysis program of the satellite.

II. "What We (Think We) Know"

In this section we list some of the reasonably well established features of the behaviour of the waves and particles in the inner magnetosphere near the equatorial plane and attempt to illustrate these features where appropriate with observations from Explorer 45.

1. The magnetospheric particle populations are subject to a decay of existing intensities and to repopulation through processes of "injection" and diffusion.

The sudden appearence of hot plasma in a region not previously populated by such plasma in the magnetosphere is easy to observe so that the concept of "injection" during the onset of each magnetospheric substorm is widely accepted. In Figs. 1–4 we present the relative intensities of electrons and protons

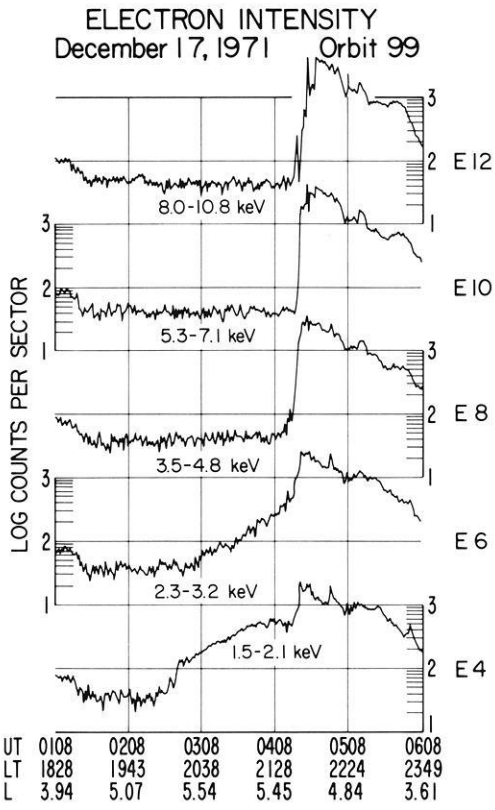

Fig. 1. Intensity of electrons from 1.5 to 10.8 keV recorded by Explorer 45 during orbit 99 near apogee on December 17, 1971 (Barfield and DeForest, 1974)

recorded when S^3 was near apogee on December 17, 1971. It will be noted that there was a sudden increase in the intensity of both electrons and protons near 0420 UT in connection with a substorm observed at about the same time on ground base magnetograms (Fig. 5) (Barfield and DeForest, 1974). This brings us to the next point.

2. During all "injection" events both electrons and protons (ions) appear in the magnetosphere.

Whenever S^3 is outside the high density cold plasma region known as the plasmasphere increases in the intensities of both electrons and ions occur during each magnetospheric substorm. This is similiar to the observations of DeForest and McIlwain (1971) on ATS-5 at $L=6.6$.

3. The inner boundary of the injection process appears to be associated roughly with the plasmapause.

In the example of the injection process given in Figs. 1–4, the satellite crossed the plasmapause at about 0200 UT ($L=4.95$) on the outbound portion of the orbit and then at about 0616 UT ($L=3.4$) on the inbound leg of the orbit according to the DC electric field experiment definition of the plasmapause. In this example the injection process appears to operate entirely outside the plasma-

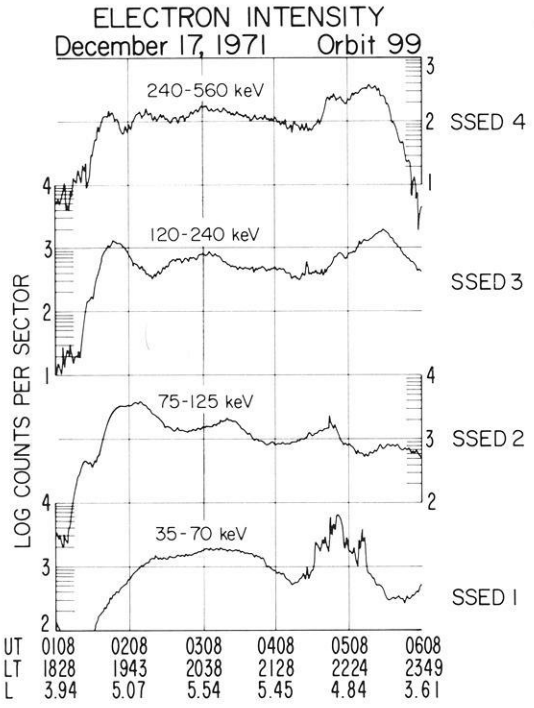

Fig. 2. Continuation of Fig. 1 for electrons from 35 to 560 keV

pause. In Figs. 16 and 17 examples (which we will discuss later) are presented in which energetic protons are injected well into the region of the plasmasphere. The inner boundary of the injected particles can appear at any distance from $L=2.0$ to the apogee of S^3 but the plasmapause is usually no more than 0.5 L away from this inner edge even on the deepest, most intense penetrations of the injection process. There can be overlap but there appears to be a rough association in the position of the two boundaries (Williams and Lyons, 1974a and b; Williams, 1974).

4. After the particles appear as a result of the "injection" process their subsequent motion is consistent with normal drifts in the combined geomagnetic and geoelectric fields present in the magnetosphere

Various features of the injected particle distributions during substorms (Konradi *et al.*, 1973; Williams *et al.*, 1974; Konradi *et al.*, 1975) and during main phase magnetic storms (Smith and Hoffman, 1973; 1974) have been explained in this manner. This is the basic approach employed successfully by McIlwain (1974) in explaining particle variations at ATS-5.

5. Convection does play a dominant role in explaining the overall gross motions of the particle dynamics.

Although other types of electric fields could contribute to the geoelectric field noted in point 4 above, the convection electric field appears sufficient to explain the overall gross motions of the particles. Maynard and Chen (1974)

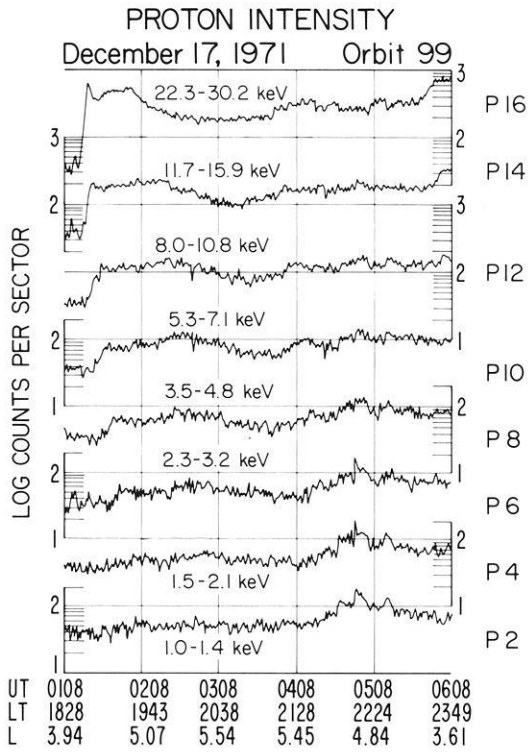

Fig. 3. Continuation of Fig. 1 for protons from 1.0 to 30.2 keV

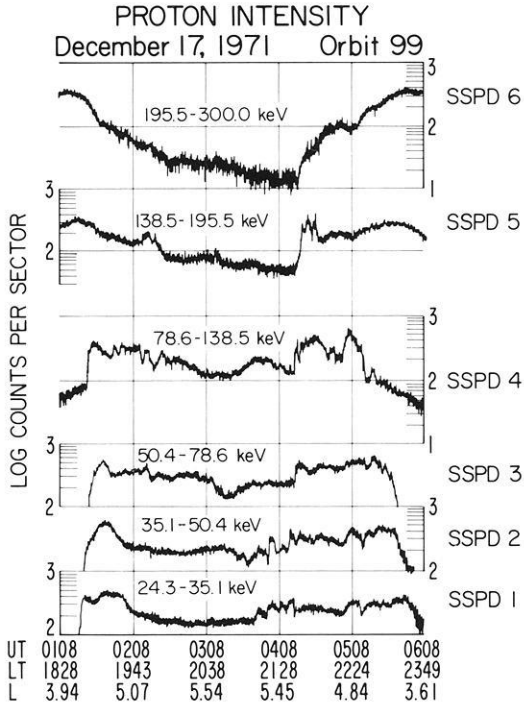

Fig. 4. Continuation of Fig. 1 for protons from 24.3 to 300 keV

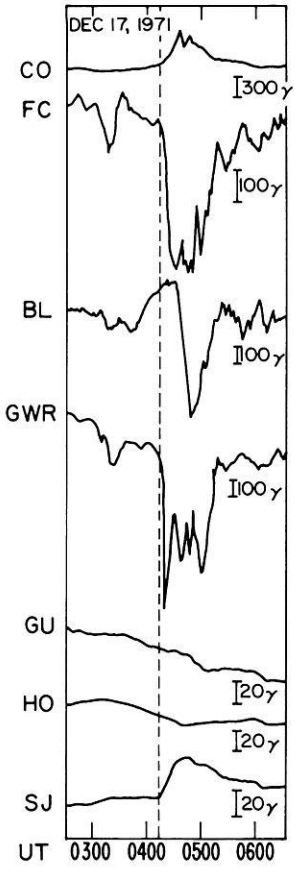

Fig. 5. Magnetograms corresponding to the time period of the Explorer 45 orbit 99 of Figures 1–4 for four high latitude stations, College (*CO*), Fort Churchill (*FC*), Baker Lake (*BL*), and Great Whale River (*GWR*) along with three low latitude stations, Guam (*GU*), Honolulu (*HO*), and San Juan (*SJ*) (Barfield and DeForest, 1974)

have studied the S^3 observations of detached cold plasma regions and confirm that convection is the basic underlying process in the formation of these regions but find that more localized processes are needed to explain the observed detailed structure of these regions. Barfield *et al.* (1975) have studied the development of a single detached cold plasma region and come to similiar conclusions.

6. During intense "injection" events the populations of ions, particularly protons from 10 keV to 100 keV are enhanced to produce a "storm-time" ring current.

Explorer 45 is providing the first total proton energy density measurements in the storm-time ring current region. These observations show that the stormtime ring current is produced by the injection of protons with energies from 1 keV to 140 keV with particles from 10 keV to 60 keV producing the largest increase from the quiet time distribution (Hoffman, 1973; Smith and Hoffman, 1973, 1974; Fritz *et al.*, 1974). An example of the proton spectral changes which occur during an intense proton injection leading to the production of a strom-time ring current is presented in Fig. 6.

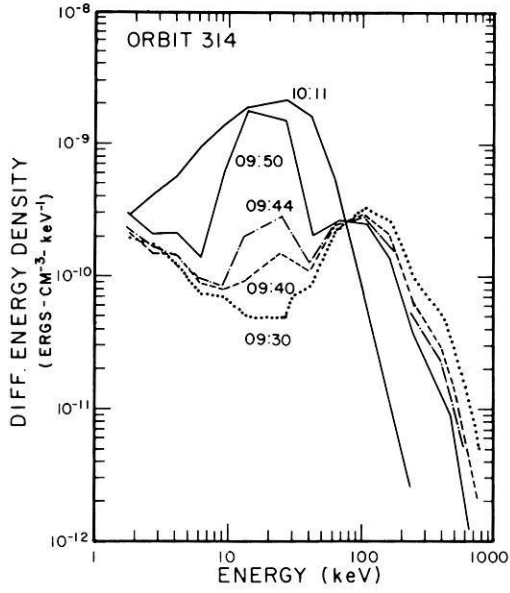

Fig. 6. The evolution of the energy density spectrum of protons as a function of radial distance on the outbound portion of Explorer 45 orbit 314 taken during the period of the main phase decease of the geomagnetic storm beginning on February 24, 1972 (Smith and Hoffman, 1974; Fritz *et al.*, 1974)

7. The plasmasphere is filled with an emission called ELF hiss much of the time. This hiss appears to have been produced at a specific location and then propagates to fill a larger portion of the plasmaspheric volume.

Plasmaspheric hiss has been observed for some time (Russell and Holzer, 1970). An extensive study of the occurrence of this ELF hiss along the S^3 orbit has been performed by Parady *et al.* (1974). Although there are large intensity variations they found hiss in the frequency range from 100 Hz to 1000 Hz on 108 of 112 orbits which they examined. For most orbits the hiss occurred inside the S^3 determination of the plasmapause. There were cases, however, when the hiss definitely extended to radial distances outside of the S^3 plasmapause determination but these could have been cases of a very gradual transitions from the low to high density cold plasma regions. A textbook type of example of the behaviour of this hiss is presented in Fig. 7 (Anderson and Gurnett, 1973). On this inbound S^3 pass electrostatic noise was observed up to the sharp plasmapause crossing at 0615 UT. As the plasmasphere was entered a strong, unstructured hiss emission appeared in the band from 300 Hz to 400 Hz in both the electric and magnetic field wideband data. This transition region is presented in greater detail in Fig. 8. The ELF hiss band was spin modulated and it had the same well defined frequency limits for more than 30 minutes as the satellite moved inward more than one earth radii in distance. By analyzing the spin modulation Anderson and Gurnett (1973) were able to determine that the propagation direction of the hiss was nearly normal to the local magnetic field direction. The invariance of the frequency limits observed and the propagation direction strongly suggest that the hiss was being generated within a localized region and then propagating to other regions of the plasmasphere.

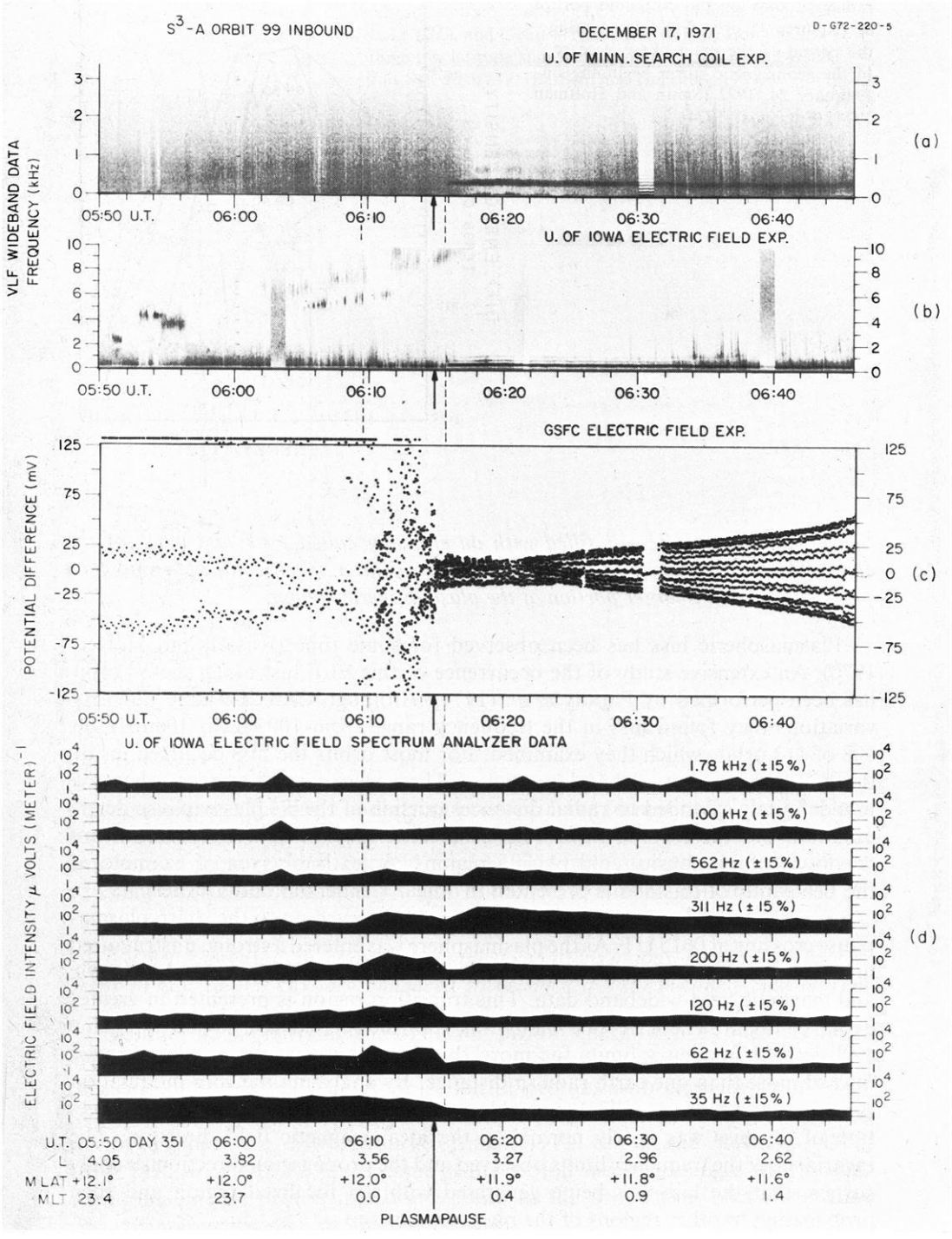
S3-A ORBIT 99 INBOUND
DECEMBER 17, 1971
D-G72-220-5
U. OF MINN. SEARCH COIL EXP.
VLF WIDEBAND DATA FREQUENCY (kHz)
(a)
05:50 U.T.
06:00
06:10
06:20
06:30
06:40
U. OF IOWA ELECTRIC FIELD EXP.
(b)
GSFC ELECTRIC FIELD EXP.
POTENTIAL DIFFERENCE (mV)
(c)
U. OF IOWA ELECTRIC FIELD SPECTRUM ANALYZER DATA
ELECTRIC FIELD INTENSITY μ VOLTS (METER)-1
1.78 kHz (±15%)
1.00 kHz (±15%)
562 Hz (±15%)
311 Hz (±15%)
200 Hz (±15%)
120 Hz (±15%)
62 Hz (±15%)
35 Hz (±15%)
(d)
U.T. 05:50 DAY 351
L 4.05
3.82
3.56
3.27
2.96
2.62
M LAT +12.1°
+12.0°
+12.0°
+11.9°
+11.8°
+11.6°
MLT 23.4
23.7
0.0
0.4
0.9
1.4
PLASMAPAUSE

8. The behaviour of energetic electrons ($E \gtrsim 40$ keV) inside the plasmapause is reasonably well understood. With periodic substorm injections of electrons occurring in the vicinity of the plasmapause, the two-zone structure (inner and outer zone), relative intensities as a function of energy, and pitch-angle distributions of energetic electrons can be explained by balancing radial diffusion with losses from atmospheric coulomb collisions and from pitch-angle diffusion resulting from resonant interactions with the known whistler-mode plasmaspheric hiss noted in point 7.

Rather than attempt a completely self-consistent calculation of wave generation and the resulting particle diffusion, Lyons *et al.* (1972) used a distribution of whistler-mode waves modelled after the observed plasmaspheric hiss spectrum and calculated diffusion coefficients for particle resonances with this spectrum. Examples are shown in Fig. 9 for electrons with three different electron energies at $L=4$. By including all cyclotron harmonic resonances including the Landau (zeroth order) reasonances along with the effects of geomagnetic field gradients, Lyons *et al.* (1972) predicted that the pitch angle distributions of energetic electrons would display a significant bump near 90° equatorial pitch angle due to the relatively slow diffusion rates within the pitch angle range of overlap between the cyclotron and Landau reasonances. The size of this bump should decease with increasing electron energy since the cyclotron resonance extends to increasingly larger pitch angles with increasing electron energy. For a given energy the size of the bump should also decrease with increasing L since the minimum parallel electron energy for which cyclotron resonance can occur decreases with L. Explorer 45 observations of electrons (30 keV to 560 keV) show that such pitch angle distributions (Fig. 10) with the predicted variation with L and energy are a normal feature of the quiet time radiation belts (Lyons and Williams, 1974a). The shape of the pitch angle distributions is greatly perturbed during storm-time injections. Following such injections the Explorer 45 observations show that the quit time pitch angle distributions gradually reform (Lyons and Williams, 1974b).

Lyons and Thorne (1973) were able to calculate the fluxes of electrons as a function of energy and L and to give an explanation for the two-zone, quiet time structure of the radiation belt electrons by balancing pitch angle scattering and coulomb collision losses with inward radial diffusion driven by substorm associated fluctuations of the convection electric field from an average outer zone source. The resulting equilibrium structure is expected to be steady during quiet times except in the outer regions of the plasmasphere where the fluxes vary somewhat during quiet times in response to substorm activity. This is the

◀ **Fig. 7.** Four sets of field observations for inbound Explorer 45 orbit 99 in the vicinity of the plasmapause. All four panels contain data for the same 56 minutes time period from 0550 to 0646 UT on December 17, 1971. Panel (a) is a 0-Hz to 3-kHz frequency-time spectrogram of the magnetic field wideband data. Panel (b) is a 0-Hz to 10-kHz frequency-time spectrogram of the electric field wideband data. Panel (c) is a plot of the dc potential difference between the spheres of the DC electric field experiment (Maynard and Cauffman, 1973). Panel (d) contains plots of the peak amplitudes measured for the eight lowest frequency channels of the University of Iowa's electric field experiment on board spectrum analyzer (Anderson and Gurnett, 1973)

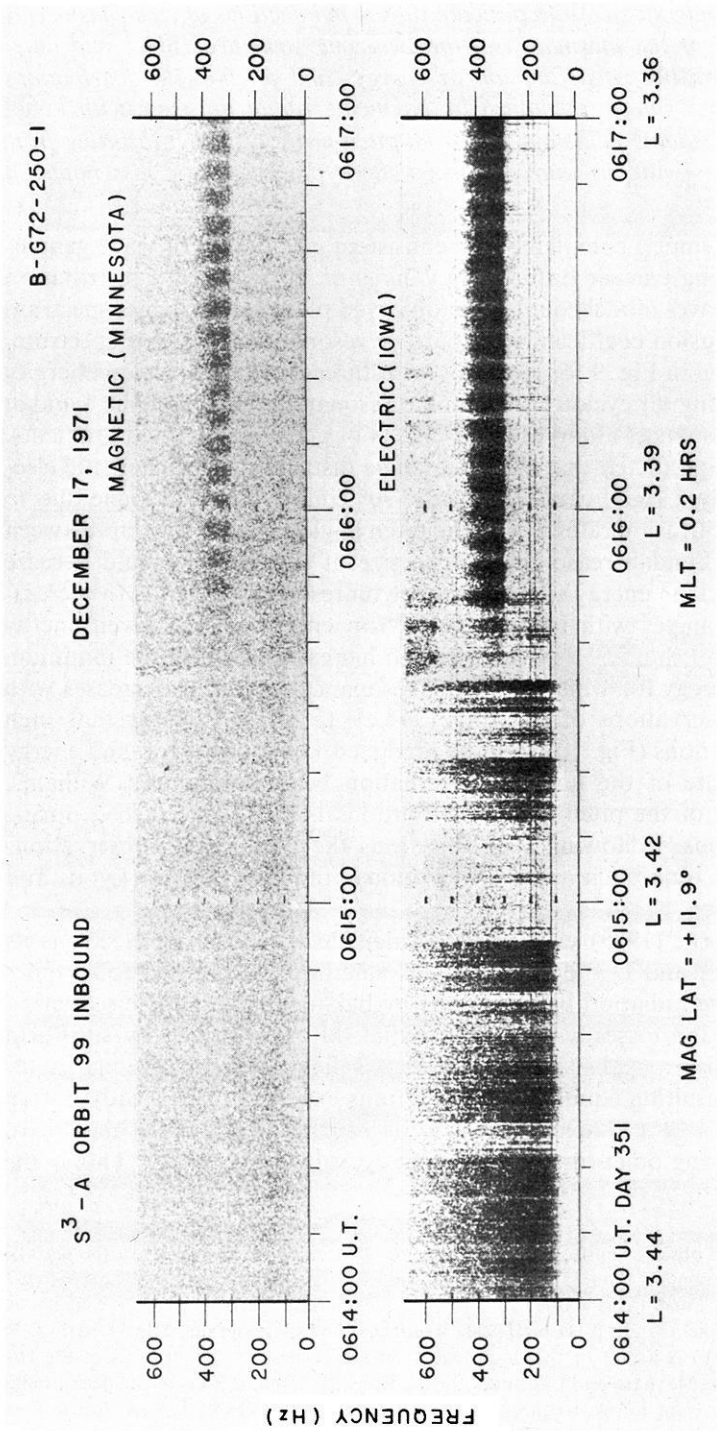

Fig. 8. An expanded portion of Explorer 45 orbit 99 presented in Fig. 7. The upper panel is a 0- to 650-Hz frequenzy-time spectrogram of the magnetic field wideband data. The lower panel is a 0- to 650-Hz frequency-time spectrogram of the electric field wideband data. Both panels are for the same 3-min period near the plasmapause. Note that the intense vertical bursts from 06h14m00s to 06h15m40s UT occur only in the electric field data. The ELF hiss band from about 300 to 420 Hz, which begins at 06h15m37s UT, is present in both the electric and the magnetic field data. Analysis of the spin modulation of the ELF hiss band determined that the hiss is propagating nearly perpendicular to the geomagnetic field. The ELF hiss band has the same well-defined frequency for more than 30 min as the satellite moves inward more than 1 R_E (Anderson and Gurnett, 1973)

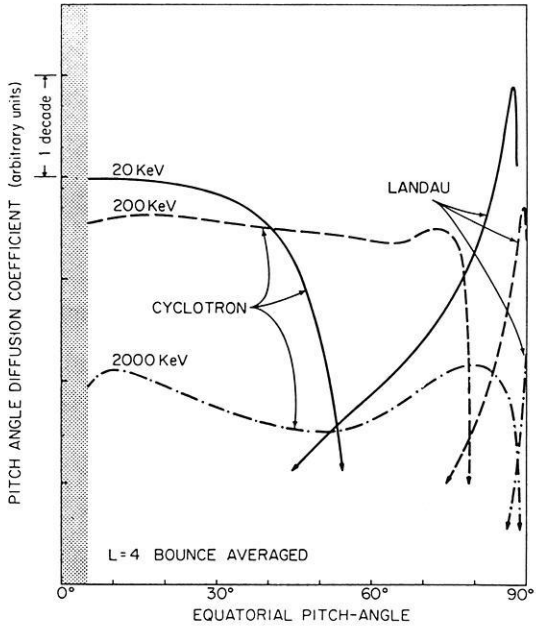

Fig. 9. Bounce orbit averaged cyclotron and Landau resonant pitch angle diffusion coefficients as a function of equatorial pitch-angle at $L=4$ for 20, 200, and 2000 keV electrons. (Lyons *et al.*, 1972)

behaviour shown in Fig. 11 for Explorer 45 observations during quiet times. The theory was able to predict the measured overall structure correctly to about an order of magnitude during the quiet time of December 9–16, 1971 (Fig. 12) which is about the order of agreement expected based on the accuracy and average character of the input parameters required by the theory (Lyons and Williams, 1974a). Following storm-time injections electron fluxes should and do decay slowly back to the pre-storm quiet-time equilibrium structure (Lyons and Williams, 1974b).

III. "What We Do not Know" and Insights Based on S^3 Observations

We now turn to a tabulation of a few of the major topics concerning the behaviour of the waves and particles in the inner magnetosphere about which there is little consensus.

1. What is the nature of the injection process? More specifically, what roles do the processes of in situ acceleration and enhanced convection play in the substorm injection process?

2. What is the actual mechanism producing the plasmaspheric hiss?

3. What roles do the various competing processes play in the decay of the storm-time ring current?

4. What role do the various species of ions play in the magnetospheric processes?

Recent results from the study of Explorer 45 observations have yielded significant insight into each of the questions tabulated above.

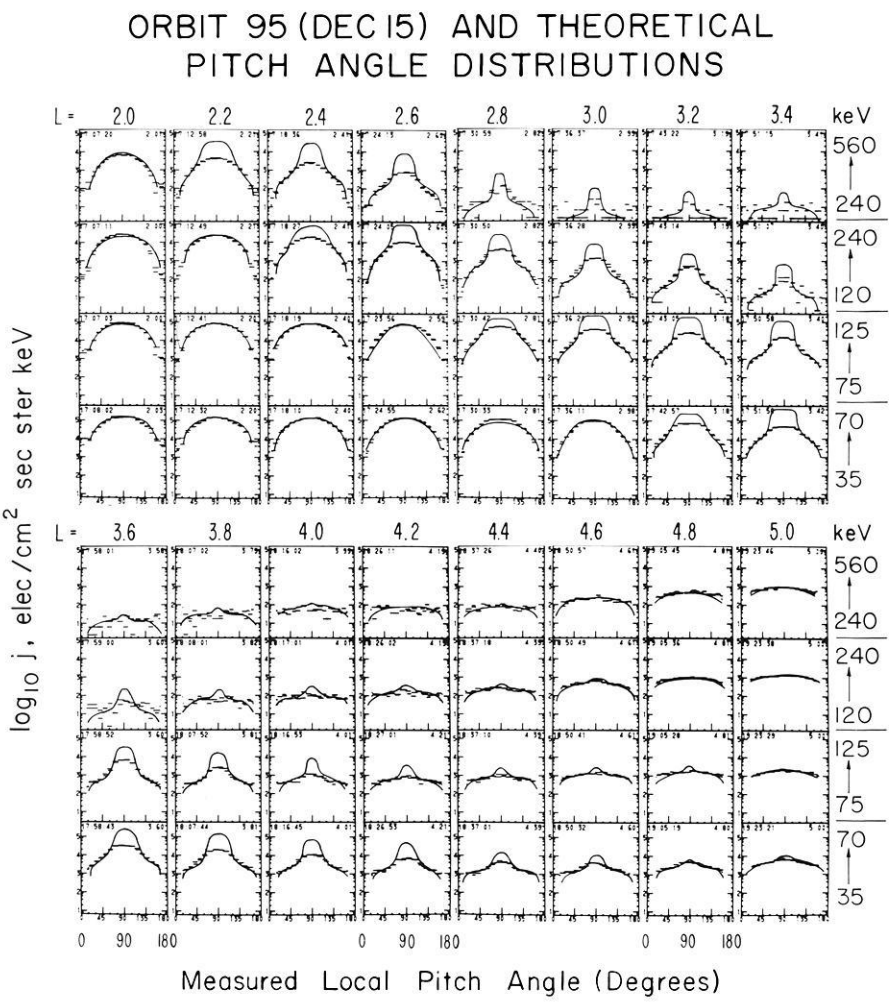

Fig. 10. Equatorial pitch angle distributions observed on Dec. 15, 1971 (orbit 95) and those predicted by Lyons *et al.* (1972) to result from resonant interactions with the plasmaspheric whistler-mode wave band. Distributions are shown every 0.2 in L from $L=2$ to $L=5$, and the four energies are stacked vertically at each L with the lowest energy at the bottom. The dashes give the measured electron flux with their horizontal extend indicating the pitch angle scan for each measurement. The solid curves are the theoretically predicted pitch angle distribution for the geometric mean energy of each energy interval. Diffusion from Coulomb collisons has been added to the theoretical calculations to account for the rounding of the pitch angle distributions within the inner zone. The vertical positionings of the theoretical distributions are arbitrary on a logarithmic scale and have thus been adjusted to best illustrate the comparison with the observations. (Lyons and Williams, 1974a)

The Injection Process

With a single satellite making observations at a single point in space it is difficult to separate effects due to space and/or time in attempting to delineate the features

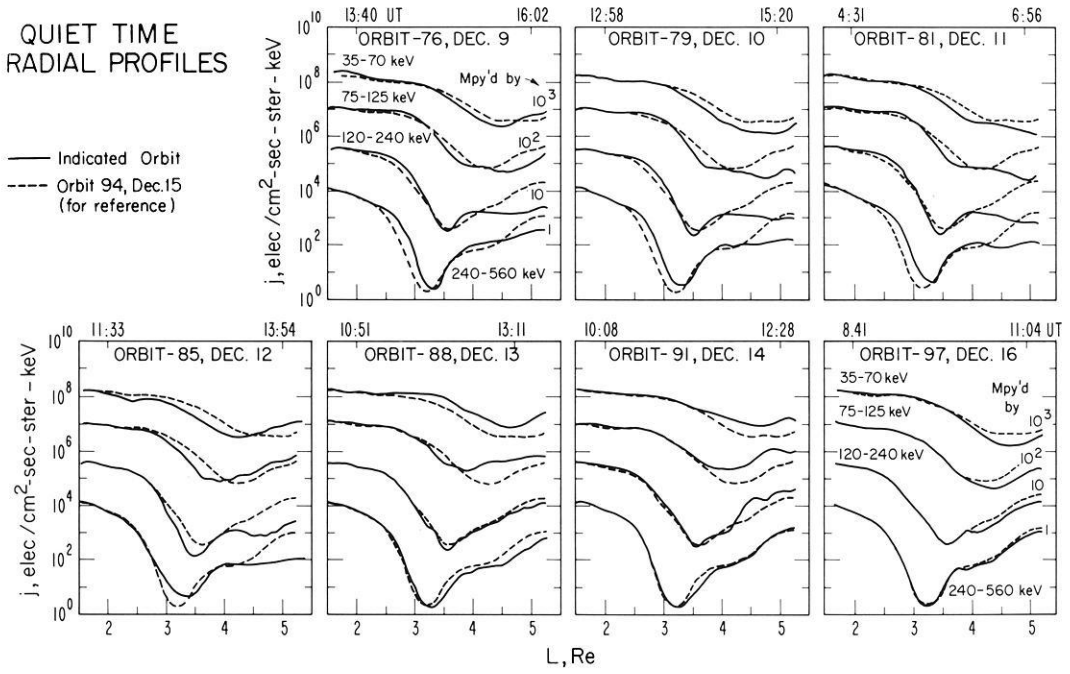

Fig. 11. Radial profiles of the perpendicular (90° local pitch angle) electron flux obtained near the geomagnetic equator, approximately once per day, for the quiet period of Dec. 9–16, 1971. Solid curves give the profiles from the orbit indicated in each panel, while the dashed curves (shown for reference) give the profiles from orbit 94 on December 15, 1971. To clearly display the data, the 120–240 keV, 75–125 keV, and 35–70 keV fluxes have been multiplied by 10^1, 10^2, and 10^3, respectively. (Lyons and Williams, 1974a)

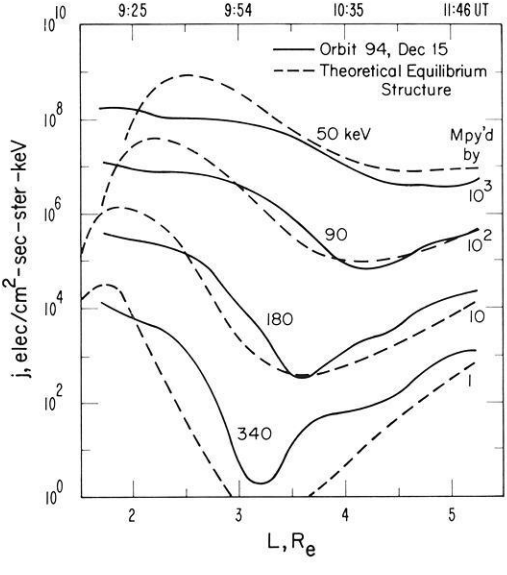

Fig. 12. Comparison between the radial profiles observed on the outbound portion of orbit 94 on Dec. 15, 1971 (solid lines) and the theoretical equilibrium radial profiles (dashed lines) as obtained from the analysis of Lyons and Thorne (1973) using $Bw = 10\,m\gamma$, $E = 0.05\,mV/m$, and an average outer zone electron energy spectrum. The theoretical profiles are for the indicated energies, which are the geometric mean of the four Explorer 45 energy channels. The 180 keV, 90 keV, and 50 keV fluxes have been multiplied by 10^1, 10^2, and 10^3 respectively. (Lyons and Williams, 1974a)

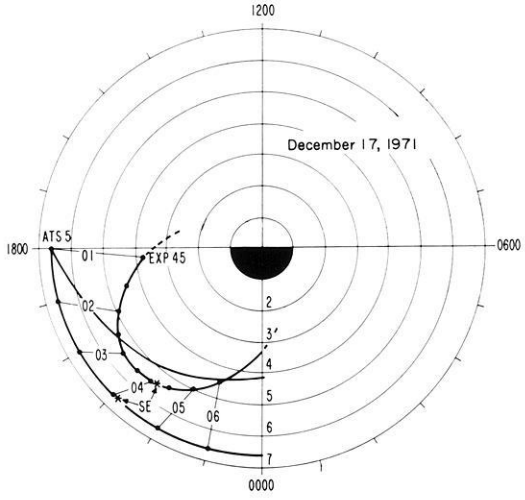

Fig. 13. The trajectories of the ATS-5 and Explorer 45 satellites in an L-value versus local time plot during the period of the substorm injection on December 17,1971 presented in Figs. 1 through 5. (Barfield and DeForest, 1974)

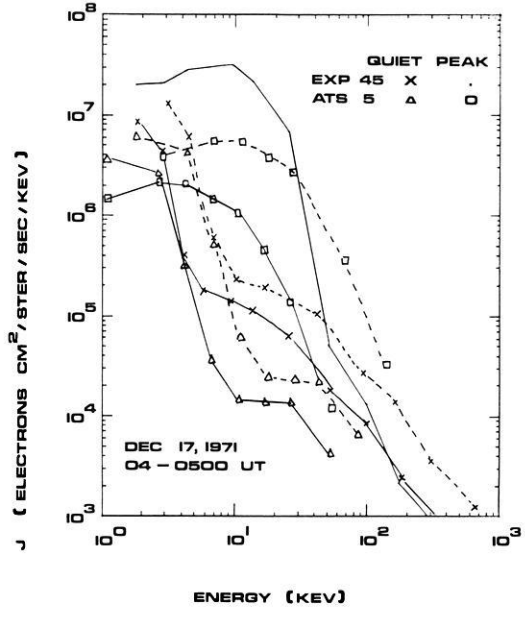

Fig. 14. Energy spectra obtained from the ATS-5 and Explorer 45 satellites during the substorm injection period of December 17, 1971 presented in Fig. 1 through 5. The solid curves represent the actual observations while the dashed curves are representative computed spectra. The dashed "quiet" curves represent the spectra obtained at the position of each sattelite by transforming in phase space from ambient conditions just prior to the substorm to those at the peak epoch. The dashed "peak" ATS-5 curve represents the transformation of the ATS-5 spectrum observed at peak epoch to the position of Explorer 45

of the substorm injection process. During the occurrence of the substorm injection event presented in Figs. 1–5, the ATS-5 satellite at geostationary orbit was in the vicinity of Explorer 45. In Fig. 13 the positions of the two satellites as a function of time are presented. The substorm enhancement (labelled as "SE" in Fig. 13) occurred when the satellites were near their point of closest approach. The "injection boundary" described by Mauk and McIlwain (1974) and by McIlwain (1974) is shown for reference in Fig. 13. Barfield and DeForest (1974)

have attempted to correlate the flux variations at the position of the satellites. In Fig. 14 the electron energy spectrum both before and at the peak of the injection event is presented for the two satellites (solid curves). Barfield and DeForest (1974) have then adiabatically transformed the spectrum recorded at each satellite prior to the event to conditions existing at the peak of the event (dashed curves with "quiet" symbols) using Liouville theorem. It is seen that effects other than those which can be attributed to adiabatic changes occurred at each satellite. In a similiar manner the spectrum recorded at ATS-5 at the peak of the event was transformed to the position of Explorer 45 (dashed spectrum with square symbols). The spectrum at Explorer 45 following the injection (solid curve without symbols) demonstrates a large excess of low energy particles and an absence of higher energy particles from what would be expected on the basis of the measured ATS-5 spectrum transformed to the position of S^3. This result is open to varying interpretations but is strongly suggestive of a non-adiabatic change in the electron distribution function occurring in the vicinity of the satellite in connection with this injection event as opposed to simple enhanced convection "injecting" the particles into the vicinity of the two satellites.

The Source Mechanism for Plasmaspheric Hiss

One of the most promising mechanisms for the production of the plasmaspheric hiss recently proposed by Thorne *et al.* (1974) involves electrons with energies from 10 to 100 keV and is schematically illustrated in Fig. 15. Prior to a substorm, electrons of these energies follow drift paths which are approximately circular (dashed lines). These paths lie outside the plasmapause at dawn but enter the asymmetric bulge of the plasmasphere in the afternoon sector where modest hiss can be produced through the cyclotron resonance mechanism proposed by Kennel and Petschek (1966) due to the enhanced cold plasma density of the plasmasphere. S^3 observations of plasmaspheric hiss during periods of low magnetic activity indicate that there is a maximum in the intensity in the afternoon (Parady *et al.*, 1974). This mechanism is consistent with generation of the hiss at a specific location (Fig. 8) as indicated in Section II (Anderson and Gurnett, 1973) and that the source is in the outer plasmasphere (Parady *et al.*, 1974).

During a substorm intense convection electric fields modify the drift orbits of these medium energy (< 100 keV) electrons (solid lines in Fig. 15) and prevent them from entering the evening plasmasphere thus causing a reduction in hiss intensity at dusk. When the convection electric fields subside electrons again follow circular drift paths and strong hiss is expected near dusk as intense fluxes of substorm-injected electrons drift into the plasmaspheric bulge (Thorne *et al.*, 1974). Using Explorer 45 electron flux observations made in the bulge region of the plasmasphere, Thorne and Barfield (1974) have shown that the medium-energy electron fluxes are depressed during substorms. At substorm subsidence, the electron fluxes return at enhanced flux levels consitent with the drift of the substorm-injected electrons into the bulge. Parady *et al.* (1974) report cases of a complete drop-out of hiss occurring on some passes although they have

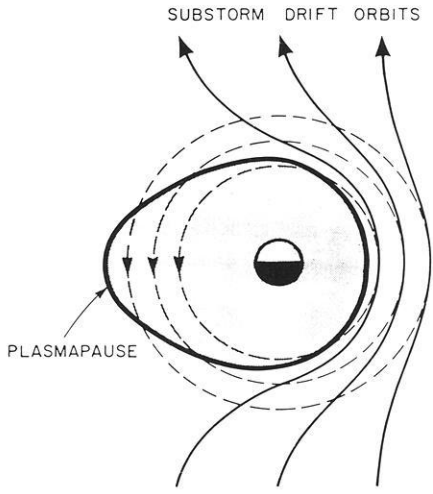

Fig. 15. A model for the generation of ELF emissions during periods of substorm activity. Before the substorm, medium energy electrons (10–100 keV) move on roughly circular (dashed) drift orbits. On entering the high density plasmasphere bulge region, cyclotron resonant energies are lowered, the resonant flux is increased and ELF hiss may be generated. During the substorm, intense convection electric fields modify the electron drift paths (solid lines). Chorus may be generated by the intense flux of injected electrons at dawn but the electrons are forbidden from entering the plasmasphere near dusk thus causing a reduction in hiss intensity. Following the substorm, electrons follow circular drift paths and intense hiss is generated near dusk. (Thorne *et al.*, 1974)

not attempted to correlate this with substorm activity. They also report that the most intense hiss is observed during the recovery phase of magnetic storms near the inner edge of the ring current. In Section II it was indicated that the inner edge of the ring current is roughly associated in position with the plasmapause so this observation is consistent with the intense hiss being produced when the newly injected electron fluxes can again drift into the plasmasphere as the convection electric field subsides. The S^3 experimenters are not in total agreement as to the source of the hiss as Parady, *et al.* (1974) have concluded that protons between 10 and 100 keV appear to be a source for some of the hiss. Parady (1974) has proposed a mechanism in which the protons produced the hiss but this mechanism appears to require anisotrophy factors which are not observed in the proton data (Lyons, personal communication) and appears to be in conflict with the observations of Thorne and Barfield (1974).

The Decay of the Storm-Time Ring Current

There are at least three major mechanisms presently under consideration which lead to the decay of the ring current proton intensities. The ion cyclotron instability as discussed by Cornwall *et al.* (1970, 1971) can operate mainly in the overlap region between the plasmapause and the inner edge of the ring current. The electrostatic loss-cone instability proposed by Coroniti *et al.* (1972) can operate

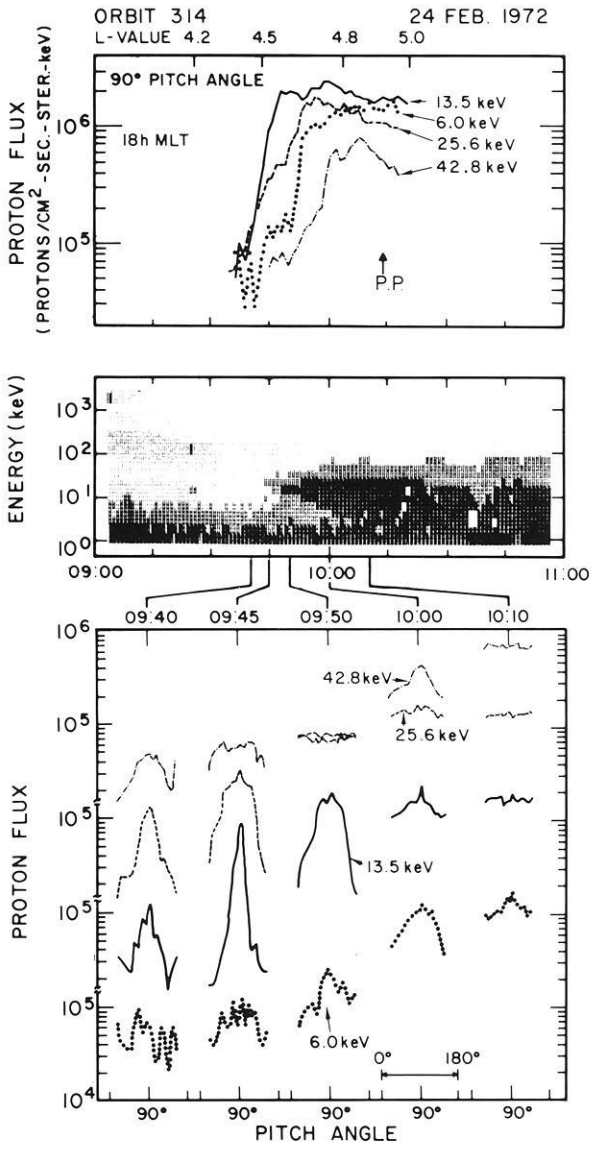

Fig. 16. Details associated with the energy build up which occurred on Explorer 45 orbit 314 presented in Fig. 6. The top panel contains profiles of four energy bands of protons whose widths are about $\pm 15\%$ around the center energies listed. The center panel contains the proton spectrogram which exhibits the nose structure described by Smith and Hoffman (1974). The grey shading is a measure of the flux (in particles/cm^2 sec ster keV) of the equatorially mirroring particles. Black represents the most intense flux. This is an unretouched computer generated plot. The lower panel contains pitch angle distributions for the same four proton energy bands as the top panel at five selected positions in the nose structure. Each pitch angle distribution consists of data from approximately 20 to 160 . (Smith and Hoffman, 1974; Fritz *et al.*, 1974)

most effectively in the region outside the high density plasmasphere. In addition to these two instabilities, charge exchange of the ring current protons with the neutral hydrogen will be ever present during the decay process.

During the injection phase of main phase magnetic storms Smith and Hoffman (1974) have observed a chracteristic of the injected proton distribution which they have named the "nose" event. In Fig. 16 the details of the injection event presented in Fig. 6 are shown. In the top panel the intensity as a function of time (L) is shown for four proton energy passbands. Note that the 13.5 keV passband is the first to increase followed first by the 25.6 keV and then the 6.0 keV passbands. This behaviour is also shown in the energy spectrogram in the middle panel. The particle energies range from 1 keV to 1000 keV and the grey shading is a measure of the intensity of the flux for 90° pitch angle protons in each energy band. The darker the shading the larger the flux. Around 1000 UT the spectrogram appears to contain a projection or "nose" and it is this feature which gives the event its characteristic name (Smith and Hoffman, 1974; Fritz *et al.*, 1974). In the bottom panel of Fig. 16 the pitch angle distributions of the various proton passbands are shown for various points in the evolution of the "nose" event. The general trend in these pitch angle distributions was an initial large increase in the 90° pitch angle intensities followed by an increase in the intensity of the lower pitch angles. Fig. 17 indicates the location along the S^3 orbit where the nose events were observed and their relationship to the plasmapause (PP), the occurrence of the storm sudden commencement (SSC),

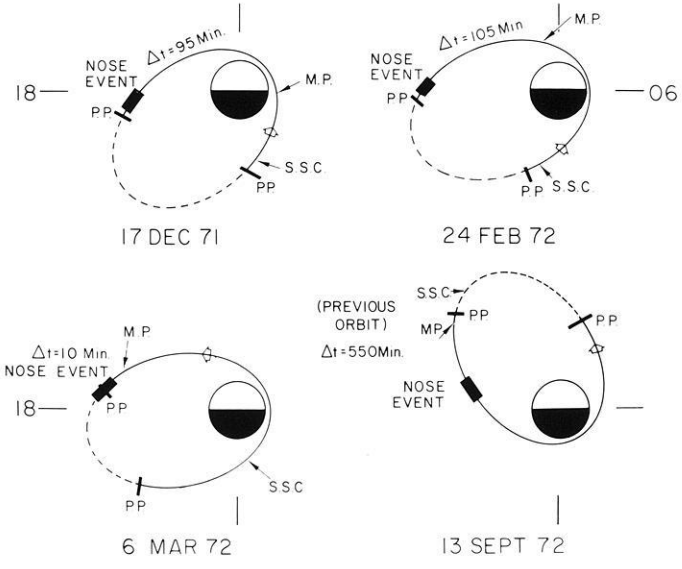

Fig. 17. The Explorer 45 orbit plotted in L and magnetic local time coordinates during four main phase magnetic storms. The positions of the satellite at the times of the storm sudden commencement (*SSC*) and the onset of the main phase decrease (*MP*) are indicated. During the portion of the orbit indicated by a dashed line the satellite was outside the measured plasmapause, indicated by the bars marked PP. The open arrow shows the direction of orbital motion of the satellite. (Smith and Hoffman, 1974; Fritz *et al.*, 1974)

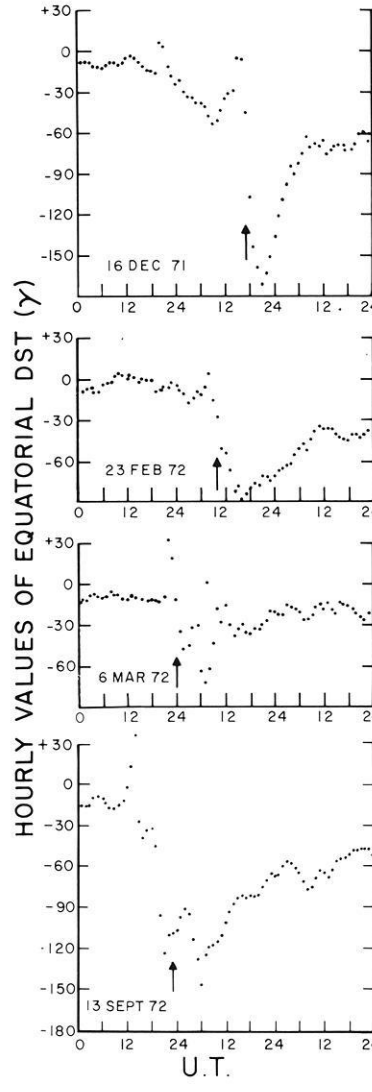

Fig. 18. $D_s t$ for the period of each of the magnetic storms studied in Fig. 17. Times of the nose structures are indicated by the arrows. (Smith and Hoffman, 1974)

and the start of the main phase decrease (MP). The quantity Δt is the time interval between the beginning of the main phase and the observation of the nose event. Fig. 18 presents the temporal relationship with $D_s t$ and shows that each of these events were observed in connection with a major magnetic storm main phase decrease. From Figs. 17 and 18 it is seen that these events (1) occur always just inside the plasmapause, (2) occur only in the local time interval near dusk, (3) occur during main phase magnetic storms but are not strongly time related to the beginning of the main phase decrease or to the sudden commencement, and (4) are independent of direction of the spacecraft being observed on both the inbound and outbound portions of the S^3 orbit.

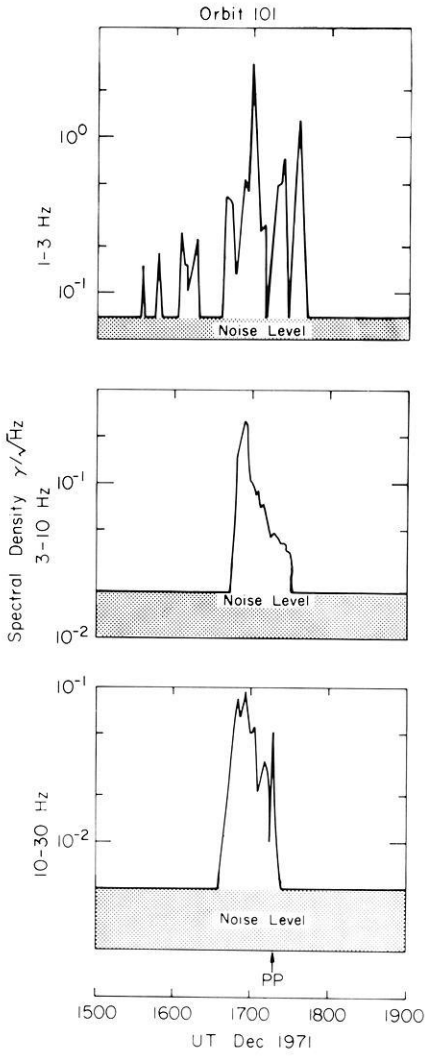

Fig. 19. Spectral densities for magnetic fluctuations in the frequency ranges 1–3 Hz, 3–10 Hz, and 10–30 Hz as measured by Explorer 45 during the outbound portion of orbit 101. The noise levels indicated are for a 30-second peak detector. (Taylor *et al.*, 1974). The plasmapause location marked is that determined by the saturation of the DC electric field experiment (Maynard and Cauffman, 1973). Orbit 101 occurred on December 17, 1971

Smith and Hoffman (1974) have explained the nose structure in the spectrogram in terms of the drift of the protons in a model magnetic and electric field. As pointed out by Roederer and Hones (1974) and more recently by Kivelson and Southwood (1974) small pitch angle particles can penetrate to smaller radial distances from the earth than the 90° pitch angle particles from their source region. The observed pitch angle distribution is just the opposite of that expected indicating that the protons with small pitch angles (large relative parallel energies) are preferentially lost.

The most likely mechanism for such a loss is the ion-cyclotron mechanism noted earlier. Taylor *et al.* (1974) has reported the observation of large amplitude (1–5 γ) waves in the frequency range < 30 Hz. These low frequency events occur very infrequently. Only ten examples were found in over 2000 hours of data. An example of one of these events is shown in Fig. 19. All events were observed

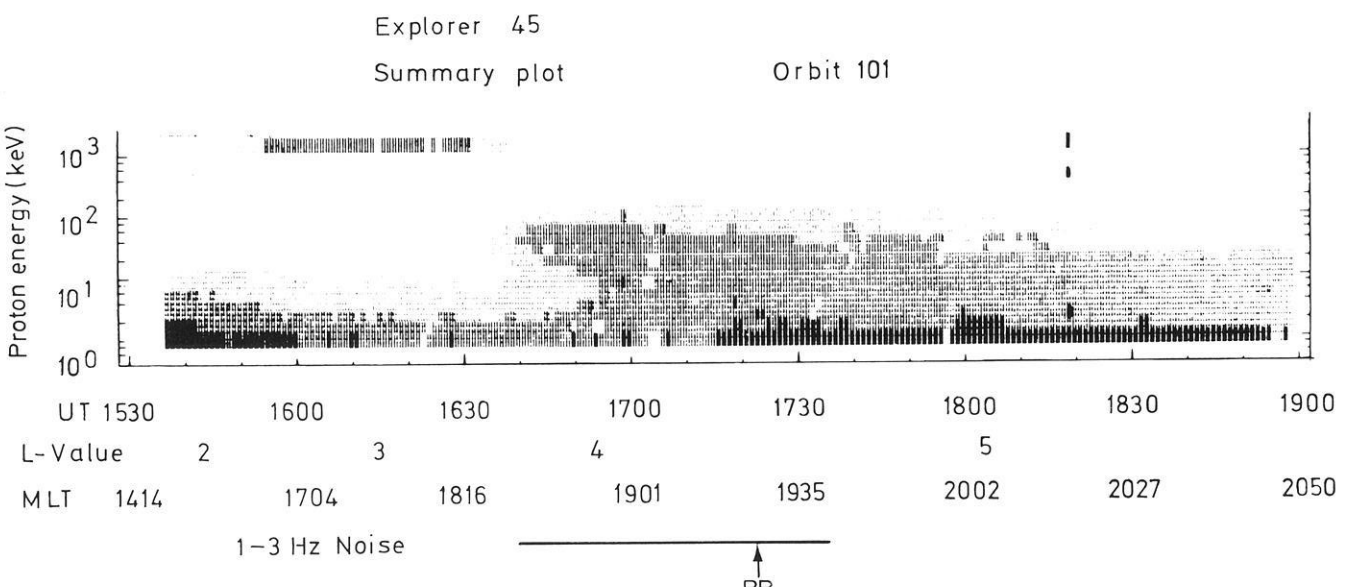

Fig. 20. An unretouched computer generated plot of the proton energy spectrogram for the outbound portion of Explorer 45 orbit 101 showing the position of the nose structure in relation to the occurrence of the 1–3 Hz noise presented in Fig. 19 and the position of the plasmapause (Taylor *et al.*, 1974). (Spectrograms are not corrected for a rate saturation effect which the solid state detectors experiment often suffers in the $2.5 \leqq L \leqq 4.0$ range so that the apparent fluxes of $24.3 \leqq Ep \leqq 201$ keV protons may be too low)

while the satellite was near the plasmapause and in the proton ring current (Taylor *et al.*, 1974).

In Fig. 20 we present another textbook-type example of the ion cyclotron instability in action. In the energy spectrogram a "nose" event is clearly seen extending well inside the plasmapause (PP). Coinciding with this overlap region the ion cyclotron 1–3 Hz noise of Fig. 19 almost perfectly covers the overlap region between the inner edge of the ring current and the plasmapause. To complete the picture developed by Cornwall *et al.* (1970 and 1971), a SAR arc was observed by the Fritz Peak observatory (Hernandez, private communication) during this time period.

In a series of studies (Williams *et al.*, 1973; Williams and Lyons, 1974a and b; Williams, 1974) the concepts of the ion cyclotron instability have been applied to explain the evolution of the proton pitch angle distributions during the recovery phase of a large magnetic storm. An example of this analysis is presented in Fig. 21. The individual plots in each figure show the observed flux versus measured local pitch angle for a particular energy and L value. Plots for all energies are stacked vertically at each L value. Sixteen energies from 1 keV to 390 keV are shown every 0.2 earth radii. Going from low to high altitudes, the pitch angle distributions evolve from rounded distributions peaked at 90° pitch angles to flat distributions, with some energies continuing their evolution to a distribution having a shallow minimum at $\alpha = \pi/2$. This structural evolution generally is seen for all energies $\lesssim 300$ keV. The change from a rounded to a flat distribution often takes place over a small radial distance ($\leqq 0.1$ earth radii) and occurs at increasing radial distances with increasing proton energies. A study of additional recovery phase orbits shows that this pattern moves to higher alititudes with time.

Although no waves < 30 Hz above the threshold of the search coil magnetometers were seen during these recovery phase orbits the transition from the flat-top to the rounded pitch angle distributions appears to result from a depletion of particles with small pitch angles in a manner similar to that described above for the ion-cyclotron instability hypothesis of Cornwall *et al.* (1970). The resonant energy equation describing the cyclotron resonance conditions for protons (Kennel and Petschek, 1966) is:

$$E_{\|,\,\mathrm{res}} = \frac{B^2}{8\pi N} A^{-2}(1+A)^{-1} = \frac{B^2}{8\pi N} F(A)$$

where B is the local magnetic field magnitude and N is the total plasma density. A is a particle anisotropy factor obtained from the pitch angle distribution function and $F(A)$ is a function of order 1 (Williams, 1974). We estimate $E_{\|,\mathrm{res}}$ as a function of altitude by observing the altitude at which the various differential energy channels begin their transition from flat-top to rounded pitch angle distributions.

This measurement of $E_{\|,\mathrm{res}}$ combined with the measured value of B allows a normalized plasma density to be calculated as a function of altitude

$$\frac{N}{F(A)} = \frac{B^2}{8\pi E_{\|,\,\mathrm{res}}} (\mathrm{cm})^{-3}.$$

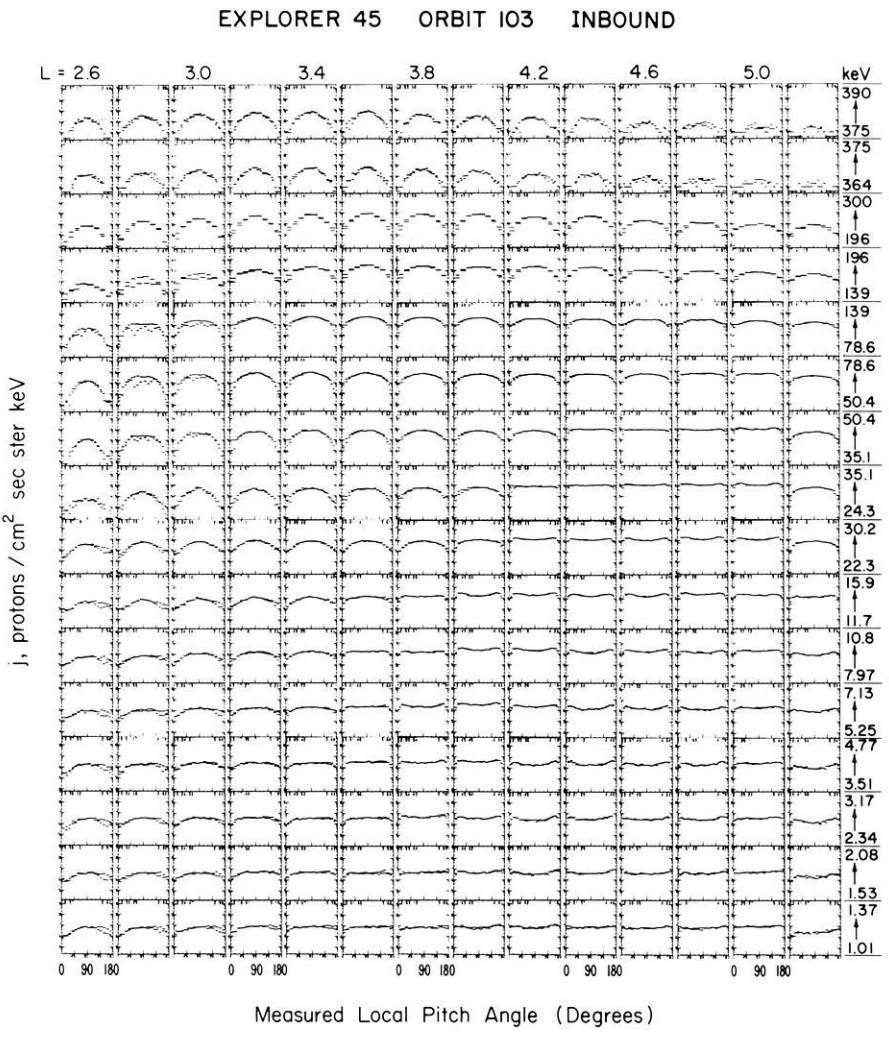

Fig. 21. Proton ring current (hot plasma population) snapshot during the December 18, 1971 storm recovery phase. Note transformation of flat-top (concave-top) pitch angle distributions to rounded pitch angle distributions peaked at 90° with lower energies transforming at lower altitudes. When pitch angle scans in the flat-top distributions reach the loss cone region, intensity decreases are seen implying an empty loss cone. Each individual plot shows $\log_{10}$ differential flux versus measured local pitch angle for a specific energy and L value. Plots for sixteen energies covering 1-390 keV are stacked at a given L value and shown every 0.2 R_E. This is a subset of the full display covering 1-872 keV and every 0.1 R_E which was used for analysis. No data editing has been done. The region where the solid state detector (24.3-300 keV) often suffers a saturation problem (Williams *et al.*, 1973) occurs for $L \lesssim 3.2$. This saturation problem appears as unusual depressions in intensities for pitch angles $90° \pm 45°$. Contamination of the channeltron instrument (1-30.3 keV) by reflected sunlight at near background count rates can be seen during the 90°-180° pitch angle sweep. This problem is related to spin axis orientation, is easily identified, and in the present data does not exist in the 0°-90° pitch angle sweep. Neither of the above effects has any influence on the present study. Data dropouts and telemetry noise effects can also easily be identified (Williams, 1974)

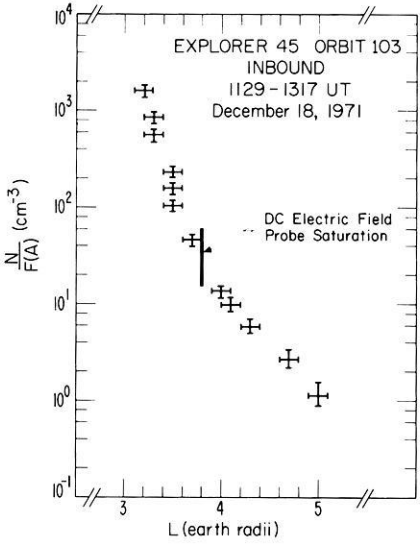

Fig. 22. Plot of $N/F(A)$ versus altitude. Resonant energy equation used to obtain $N/F(A) = B^2/8\,\pi E_{\parallel\,res}$. Altitude determined as that point where flat top distributions begin their transformation to a rounded distribution. Altitude and density estimate of DC electric field probe saturation is shown. This analysis strongly indicates that the moderate pitch angle diffusion responsible for the rounded pitch angle distribution is due to the amplification of ion-cyclotron waves as the hot ring current plasma interacts with the cold plasmaspheric plasma in the region of the plasmapause (Williams, 1974)

The result of this calculation is shown in Fig. 22 for the orbit presented in Fig. 21. The in situ estimate of the plasma density obtained from the saturation of the DC electric field experiment (Maynard and Cauffman, 1973) is also shown. The agreement is good and the inferred plasmapause shape is quite reasonable.

Additional orbits in this sequence have been analyzed in order to investigate the time behaviour of the $N/F(A)$ boundary. These results are shown in Fig. 23. The apparent outward motion is consistent with average plasmaspheric refilling rates of $\sim 2\times 10^8$ ions/cm^2 sec at $L=3.5$ to $\sim 2.5\times 10^7$ ions/cm^2 sec at $L=4.5$ (Williams, 1974). These refilling rate estimates are in agreement with earlier observations by Chappell *et al.* (1970) and Park (1970) and with the theoretical expectations of Banks (1972).

Therefore we conclude that the ion cyclotron instability as proposed by Cornwall *et al.* (1970) does operate in the vicinity of the plasmapause during main phase magnetic storms.

Low altitude results reported by Hultqvist (Hultqvist, 1974a; Bernstein *et al.*, 1974; Hultqvist, 1974b) indicate that only a small fraction of the total proton precipitation into the atmosphere occurs inside the position of the plasmapuse. This indicates the necessity of requiring a second mechanism such as the electrostatic loss cone instability proposed by Coroniti *et al.* (1972) to operate in the region well outside the region of the plasmapause. Other low altitude observations (Mizera, 1974) indicate that only of the order of 1% of the total proton energy density in the ring current particle distribution is lost in the form of precipitating protons of ring current energies into the atmosphere.

Charge exchange is a loss mechanism which operates throughout the trapping regions. Although the three dimensional density profile for neutral hydrogen to high altitudes around the earth is not well known, results exist showing the importance of charge exchange effects on storm and substorm associated protons (Swisher and Frank, 1969; McIlwain, 1972; Smith *et al.*, 1974). Fig. 24 from

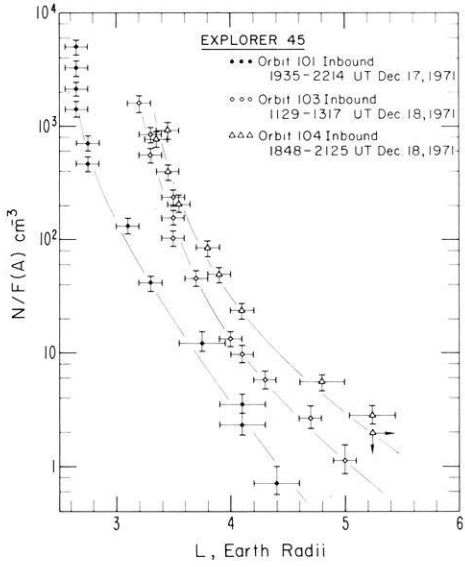

Fig. 23. Same as Fig. 22 with orbits 101 and 104 added. Outward motion of $N/F(A)$ boundary is clearly seen and is consistent with expected plasmaspheric cold plasma refilling rates

Smith *et al.* (1974) shows a comparison of the decay of proton intensities locally mirroring near the equator at various energies with the predictions due to the charge exchange process at $L=4.25$. In this case the agreement between observations and theory is very good.

Williams (1974) has qualitatively illustrated the complimentary nature of the ion cyclotron and charge exchange loss processes for the ring current during recovery phase. This is shown in Fig. 25. The horizontal bar qualitatively shows in relation to the plasmapause region what the relative strengths of charge exchange (CE) and ion cyclotron resonance (IC) losses are. The bar shows the situation for only one energy and pitch angle and will move up and down the figure for other energy-pitch angle combinations. The IC region is extended to overlap the CE region within the plasmasphere because of possible parasitic precipitation effects which may compete with charge exchange time scales (Lyons and Thorne, 1972). The shaded IC region moves left and right in accordance with the time varying plasma density profile in the plasmapause region. No other losses are included.

It is apparent that the hot plasma distribution function is dominated by the ion cyclotron resonance effect in the plasmapause region. However, the specific effects to be observed at altitudes above the plasmapause region will depend critically on the relative values of charge exchange lifetimes and plasmasphere refilling times. Well inside the plasmapause region, the remainder of the hot plasma distribution should be dominated by charge exchange and Coulomb losses. Significant hot plasma intensity exists inside the plasmapause region during recovery phase, presumably because the ion cyclotron interaction initiates only a moderate pitch angle diffusion mode and is relatively inefficient at removing particles near $\alpha \sim \pi/2$. The arrest of the instability at a moderate diffusion level may be due to absorption of wave energy by cold electrons (Cornwall *et al.*,

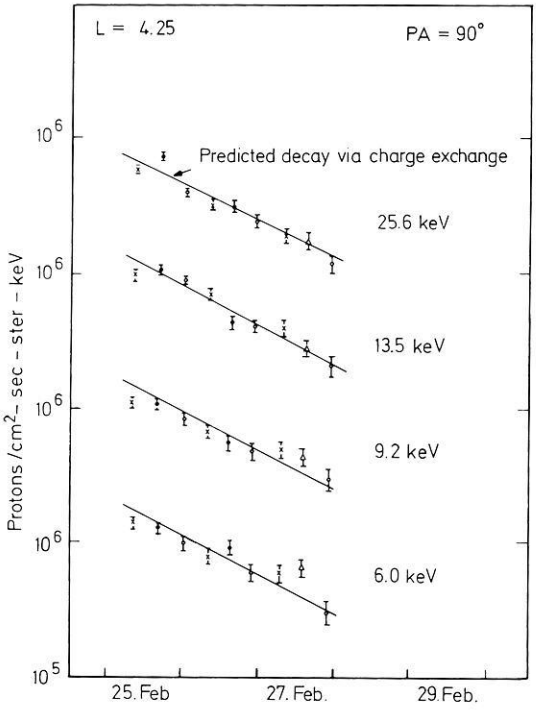

Fig. 24. Proton flux decay for particles mirroring near the equatorial plane at $L=4.25$ and local times around 2000 hours following the magnetic storm of February 24, 1972. Dst for this event is shown in Fig. 18. Fluxes measured at four energies from 6.0 to 25.6 keV are shown. The solid lines have the charge exchange decay slopes (Liemohn, 1961) for these energies at this pitch angle and L-value (Smith *et al.*, 1974)

1971) and by quenching effects due to attainment of large ratios of cold plasma density to hot plasma density (Cuperman and Landau, 1974; Cuperman *et al.*, 1973).

Williams (1974) has also shown data indicating loss rates in excess of charge exchange losses occurring at the beginning of the geomagnetic storm recovery phase. Therefore, it seems that in order to explain initial recovery phase effects as well as the low altitude observations mentioned above, additional loss mechanism have to be invoked. Furthermore, all the considerations concerning losses of the ring current during recovery phase apply to hot plasmas for which $\beta \leqq 1$. The situation for $\beta > 1$ is yet to be experimentally studied in detail and quantitatively explained theoretically.

The Role of Ions ($Z \geqq 2$) in the Magnetosphere

One of the least expected observations made by Explorer 45 was that of an intense flux of energetic ions ($Z \geqq 2$) confined closely to the geomagnetic equatorial

plane (Fritz and Williams, 1973). These ions which appear to be alpha particles, peak in intensity in the vicinity of $L = 3.5$ and could make an appreciable contribution to the "quiet-time" ring current. Recent results obtained by the Lockhead group (Shelly *et al.*, 1974 and references therein) at low altitudes indicate that energetic ions heavier than protons could play a major role in the formation of various current systems flowing in the magnetosphere such as the storm-time ring current. Almost all instrumentation flown aboard satellites in the past has not been designed to differentiate between protons and heavier ions. Very few investigations have attempted to study the potentially important role of ion species other than H^+ in magnetospheric processes. Further studies both those involving instrumentation and those involving theoretical investigations should attempt to investigate the possible role of multiple species of ions which can be involved with wave-particle interactions.

IV. Conclusions

We have attempted to indicate the existence of two wave-particle instabilities in the vicinity of the plasmapause region, the mechanism of Kennel and Petschek (1966) operating in the afternoon hours on tens of keV electrons and the mechanism of Cornwall *et al.* (1970, 1971) operating in the evening hours on tens of keV ring current protons. While these mechanisms appear to modify the distribution function of the particular particles of a given energy participating in the instability, neither mechanism appears to be a dominant loss process for the overall distribution of those particular particles.

The mechanism of Kennel and Petschek (1966) may be responsible for the production of ELF hiss which propagates to fill the region of the plasmaspheric

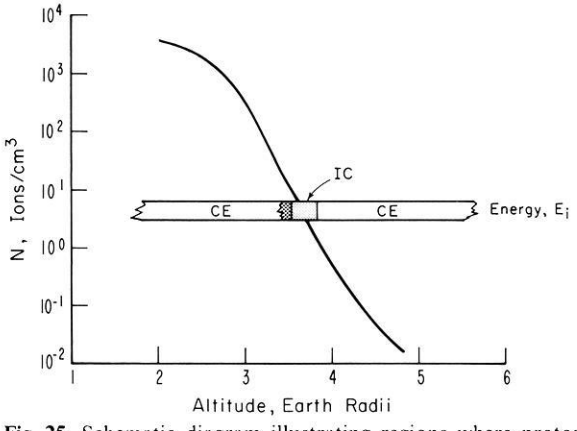

Fig. 25. Schematic diagram illustrating regions where proton flux decay due to charge exchange (*CE*) and ion-cyclotron resonance (*IC*) losses are expected to occur. Situation illustrated for one specific energy, E_i, and pitch angle. Horizontal bar moves up and down (up for lower energies) for other energy-pitch angle combinations. As cold plasma refilling occurs, plasmapause region and shaded IC region move towards higher altitudes. Overlap region illustrates extension of IC region through possible parasitic precipitation effects. No other losses are considered here. (Williams, 1974)

volume. The ELF hiss appears to be present almost all of the time and therefore cannot be acting to precipitate the electrons which produce the hiss on a fast time scale unless the electrons are constantly replenished. The ELF hiss produced in this manner is the dominant loss mechanism for $E > 40$ keV electrons inside the plasmasphere by diffusing these electrons in pitch angle through resonant interactions. With this interaction the properties of electron fluxes throughout the plasmasphere are well understood by balancing sources (radial diffusion) with losses (resonant interactions and atmospheric Coulomb collisions).

The mechanism of Cornwall *et al.* (1970, 1971) is responsible for the production of ion cyclotron waves which produce the effect of creating enhanced electron temperature in the low altitude regions where SAR arcs are produced. The qualitative relationship of this mechanism and charge exchange is shown in Fig. 25.

Energetic proton precipitation at and inside the plasmapause represents a small fraction of the total proton flux precipitating into the atmosphere (Hultqvist, 1974a and b) and this total flux itself represents a small fraction of the total ring current energy density (Mizera, 1974) which must be dissipated in the decay of the ring current. Decay via the charge exchange process appears to be the dominant process in the decay of the storm-time ring current although other wave-particle interactions may be responsible for the precipitation of protons in the region well outside the plasmapause. Whether or not protons which mirror away from the equator (finte $v_{\|}$) are affected by charge exchange or ion cyclotron resonance depends on the relative values of charge exchange lifetimes and plasmaspheric refilling times.

Acknowledgements. We would like to acknowledge the use of results from studies using Explorer 45 data, some of which have not reached the final publication phase, of Dr. J.N. Barfield, Dr. L.J. Cahill, Jr., Dr. S.E. DeForest, Dr. D.A. Gurnett, Dr. R.A. Hoffman, Dr. A. Konradi, Dr. L.R. Lyons, Dr. N.C. Maynard, Dr. B. Parady, Dr. P.H. Smith, and Dr. W.W.L. Taylor. We are especially indebted for valuable discussions with Dr. J.N. Barfield, Dr. L.R. Lyons, and Dr. P.H. Smith about various phases of this work.

This paper is intended as a contribution to a collection of papers honoring Professor G. Pfotzer of the Max-Planck-Institut für Aeronomie on his 65th birthday. We would like to express our personal appreciation to Professor Pfotzer for the help he has given in permitting a close cooperation between our respective laboratories and in particular the special arrangements which provided for a year in residence at Lindau for one of us (TAF).

References

Anderson, R.R., Gurnett, D.A.: Plasma wave observations near the plasmapause with the S^3-A satellite. J. Geophys. Res. **78**, 4756–4764 (1973)

Banks, P.M.: Behaviour of thermal plasma in the magnetosphere and topside ionosphere. In: Critical Problems of Magnetospheric Physics, Proceedings of the Joint COSPAR/IAGA/URSI Symposium, Madrid, Spain, May 11–13, 1972, E.R. Dyer, ed., pp. 152–178. Pub. IUCSTP Secretariat, 1972

Barfield, J.N., Burch, J.L., Williams, D.J.: Substorm associated reconfiguration of the duskside equatorial magnetosphere: a possible source mechanism for isolated plasma regions. J. Geophys. Res. **80**, 47–55 (1975)

Barfield, J.N., DeForest, S.E.: Simultaneous observations of magnetospheric particle variations during substorms: Explorer 45 and ATS-5. EOS Trans. Am. Geophys. Union 55, 1016 (1974)

Bernstein, W., Hultqvist, B., Borg, H.: Some implications of low altitude observations of isotropic

precipitation of ring current protons beyond the plasmapause. Planet. Space Sci. **22**, 767–776 (1974)
Chappell, C.R., Harris, K.K., Sharp, G.W.: The morphology of the bulge region of the plasmasphere. J. Geophys. Res. **75**, 3848–3861 (1970)
Cornwall, J.M., Coroniti, F.V., Thorne, R.M.: Turbulent loss of ring current protons. J. Geophys. Res. **75**, 4699–4709 (1970)
Cornwall, J.M., Coroniti, F.V., Thorne, R.M.: Unified theory of SAR arc formation at the plasmapause. J. Geophys. Res. **76**, 4428–4445 (1971)
Coroniti, F.V., Fredricks, R.W., White, R.: Instability of ring current protons beyond the plasmapause during injection events. J. Geophys. Res. **77**, 6243–6248 (1972)
Cuperman, S., Landau, R.W.: On the enhancement of the whistler mode instability in the magnetosphere by cold plasma injection. J. Geophys. Res. **79**, 128–134 (1974)
Cuperman, S., Salu, Y., Bernstein, W., Williams, D.J.: A computer simulation of cold plasma effects on the whistler instability for geostationary orbit parameters. J. Geophys. Res. **78**, 7372–7387 (1973)
DeForest, S.E., McIlwain, C.E.: Plasma clouds in the magnetosphere. J. Geophys. Res. **76**, 3587–3611 (1971)
Fritz, T.A., Williams, D.J.: Initital observations of geomagnetically trapped alpha particle at the equator. J. Geophys. Res. **78**, 4719–4724 (1973)
Fritz, T.A., Smith, P.H., Williams, D.J., Hoffman, R.A., Cahill, L.J.: Initial observations of magnetospheric boundaries by Explorer 45 (S^3). In: Correlated Interplanetary and Magnetospheric Observations, D.E. Page, ed., pp. 485–506. Dordrecht-Holland: D.Reidel 1974
Hoffman, R.A.: Particle and field observations from Explorer 45 during the December 1971 magnetic storm period. J. Geophys. Res. **78**, 4771–4777 (1973)
Hultqvist, B.: Rocket and satellite observations of energetic particle precipitation in relation to optical aurora. Ann. Géophys. (in press) (1974a)
Hultqvist, B.: The ring current and particle precipitation near the plasmapause. Kiruna Geophysical Institute Preprint No. **74**, 304 (1974b)
Kennel, C.F., Petschek, H.E.: Limit on stably trapped particle fluxes. J. Geophys. Res. **71**, 1–28 (1966)
Kivelson, M.G., Southwood, D.J.: Approximations for the study of drift boundaries in the magnetosphere. J. Geophys. Res. (submitted for publ.) (1974)
Konradi, A., Williams, D.J., Fritz, T.A.: Energy spectra and pitch angle distributions of storm-time and substorm injected protons. J. Geophys. Res. **78**, 4739–4744 (1973)
Konradi, A., Semar, C.L., Fritz, T.A.: Substorm injected protons and electrons and the injection boundary model. J. Geophys. Res. **80**, 543–552 (1975)
Liemohn, H.: The lifetime of radiation belt protons with energies between 1 keV and 1 MeV. J. Geophys. Res. **66**, 3593–3595 (1961)
Longanecker, G.W., Hoffman, R.A.: S^3-A spacecraft and experiment description. J. Geophys. Res. **78**, 4711–4717 (1973)
Lyons, L.R., Thorne, R.M.: Parasitic pitch angle diffusion of radiation belt particles by ion cyclotron waves. J. Geophys. Res. **77**, 5608–5616 (1972)
Lyons, L.R., Thorne, R.M., Kennel, C.F.: Pitch angle diffusion of radiation belt electrons within the plasmasphere. J. Geophys. Res. **77**, 3455–3474 (1972)
Lyons, L.R., Thorne, R.M.: Equilibrium structure of radiation belt electrons. J. Geophys. Res. **78**, 2142–2149 (1973)
Lyons, L.R., Williams, D.J.: The quiet-time structure of energetic (35–560 keV) radiation belt electrons. J. Geophys. Res. (submitted for publ.) (1974a)
Lyons, L.R., Williams, D.J.: The storm and post storm evolution of energetic (35–560 keV) radiation belt electron distributions, J. Geophys. Res. (submitted to publ.) (1974b)
Mauk, H., McIlwain, C.E.: Correlation of Kp with substorm-injected plasma boundary. J. Geophys. Res. **79**, 3193–3196 (1974)
Maynard, N.C., Cauffman, D.P.: Double floating probe measurements on S^3-A. J. Geophys. Res. **78**, 4745–4750 (1973)
Maynard, N.C., Chen, A.J.: Isolated cold plasma regions: Observations and their relation to possible production mechanisms. J. Geophys. Res. (submitted for publ.) (1974)
McIlwain, C.E.: Plasma convection in the vicinity of the geostationary orbit. In: Earth's Magnetospheric Processes, B.M. McCormac, ed., pp. 268–279. Dordrecht-Holland: D. Reidel 1972

McIlwain, C.E.: Substorm injection boundaries. In: Magnetospheric Physics, B.M. McCormac, ed., pp. 143–154. Dordrecht-Holland: D. Reidel 1974

Mizera, P.F.: Observations of precipitating protons with ring current energies. J. Geophys. Res. **79**, 581–588 (1974)

Parady, B.: Measurement of low frequency magnetic fluctuations in the magnetosphere. Ph.D. Thesis, 246 pages, University of Minnesota, Minneapolis, Minnesota, March, 1974

Parady, B.K., Eberlein, D.D., Marvin, J.A., Taylor, W.W.L., and Cahill, L.J.: Plasmaspheric hiss observations in the evening and afternoon quadrants. J. Geophys. Res. (submitted for publ.) (1974)

Park, C.G.: Whistler observations of the interchange of ionization between the ionosphere and protonosphere. J. Geophys. Res. **75**, 4249–4260 (1970)

Roederer, J.G., Hones, E.W.: Motion of magnetospheric particle clouds in a time-dependent electric field model. J. Geophys. Res. **79**, 1432–1438 (1974)

Russell, C.T., Holzer, R.E.: AC magnetic field. In: Particles and Fields in the Magnetosphere. B.M. McCormac, ed., pp. 195–212. Dordrecht-Holland: D. Reidel 1970

Shelley, E.G., Sharp, R.D., Johnson, R.G.: The ionosphere as a source of ring current particles, Trans. Am. Geophys. Union **55**, 1015 (1974)

Smith, P.H., Hoffman, R.A.: Ring current particle distributions during the magnetic storm of December 16–18, 1971. J. Geophys. Res. **78**, 4731–4737 (1973)

Smith, P.H., Hoffman, R.A.: Direct observations in the dusk hours of the characteristics of the storm-time ring current particles during the beginning of magnetic storms. J. Geophys. Res. **79**, 966–971 (1974)

Smith, P.H., Hoffman, R.A., Fritz, T.A.: Ring current proton decay by charge exchange. Goddard Space Flight Center Research Report, 1974

Swisher, R.L., Frank, L.A.: Lifetimes for low-energy protons in the outer zone. J. Geophys. Res. **73**, 5665–5672 (1968)

Taylor, W.W.L., Parady, B., Cahill, L.J.: Explorer 45 observations of 1–30 Hz magnetic fields near the plasmapause during magnetic storms. J. Geophys. Res. (submitted for publication) (1974)

Thorne, R.M., Barfield, J.N.: On the origin of plasmaspheric hiss (in preparation) (1974)

Thorne, R.M., Smith, E.J., Fiske, K., Church, S.: Intensity variations of ELF hiss and chorus during isolated substorms. Geophysical Research Letters, **1**, 193–196 (1974)

Williams, D.J., Fritz, T.A., Konradi, A.: Observations of proton spectra ($1.0 \leqq Ep \leqq 300$ keV) and fluxes at the plasmapause. J. Geophys. Res. **78**, 4751–4755 (1973)

Williams, D.J.: Hot-cold plasma interactions in the earth's magnetosphere. Proceedings of the Symposium on the Magnetospheres of Earth and Jupiter, Frascati, Italy, May 28–June 1, 1974

Williams, D.J., Barfield, J.N., Fritz, T.A.: Initial Explorer 45 substorm observations and electric field considerations. J. Geophys. Res. **79**, 554–564 (1974)

Williams, D.J., Lyons, L.R.: The proton ring current and its interaction with the plasmapause: storm recovery phase. J. Geophys. Res. **79**, 4195–4207 (1974a)

Williams, D.J., Lyons, L.R.: Further aspects of the proton ring interaction with the plasmapause: Main and recovery phases. J. Geophys. Res. **79**, 4791–4798 (1974b)

Received October 28, 1974; Revised Version April 7, 1975